

Anticancer Activity of *Garcinia xanthochymus* Crude Extracts Against Human Cancer Cells: *In Vitro* Evaluation in MDA-MB-231, Huh-7, A549, and SW480 Cell Lines

Sirachuch Maungprasert¹, Wim Vanden Berghe^{2,3,4}, Chung Sub Kim^{5,6},
Surat Laphookhieo¹, Keerakarn Somsuan^{7,8}, Siripat Aluksanasuwan^{7,8},
Attthapan Morchang^{7,8} and Suwanna Deachathai^{9,*}

¹Center of Chemical Innovation for Sustainability, School of Science, Mae Fah Luang University, Chiang Rai 57100, Thailand

²Cell Death Signaling - Epigenetics Lab, University of Antwerp, Wilrijk 2610, Belgium

³Integrated Personalized & Precision Oncology Network, University of Antwerp, Wilrijk 2610, Belgium

⁴Department of Biomedical Sciences, University of Antwerp, Wilrijk 2610, Belgium

⁵School of Pharmacy, Sungkyunkwan University, Suwon 16419, Republic of Korea

⁶Department of Biopharmaceutical Convergence, Sungkyunkwan University, Suwon 16419, Republic of Korea

⁷School of Medicine, Mae Fah Luang University, Chiang Rai 57100, Thailand

⁸Cancer and Immunology Research Unit, Mae Fah Luang University, Chiang Rai 57100, Thailand

⁹School of Science, Mae Fah Luang University, Chiang Rai 57100, Thailand

(*Corresponding author's e-mail: suwanna.dea@mfu.ac.th)

Received: 4 June 2025, Revised: 23 July 2025, Accepted: 3 August 2025, Published: 20 August 2025

Abstract

Garcinia xanthochymus is a medicinal plant known for its rich content of xanthenes and flavonoids, and has gained attention for its potential therapeutic properties, including anticancer effects. This study evaluated the *in vitro* anticancer activity of crude extract from *G. xanthochymus* against 4 human cancer cell lines: MDA-MB-231 (breast), Huh-7 (liver), A549 (lung), and SW480 (colon). Extracts from barks, leaves, and twigs were prepared by maceration using 4 different organic solvents: hexanes, dichloromethane, acetone, and methanol. The metabolite profiles of the extracts were characterized using UHPLC-QTOF mass spectrometry. The effects of the extracts on cytotoxicity, apoptosis, and colony-forming capability were assessed using MTT, annexin V-FITC/PI staining, and colony formation assays, respectively. The results showed that the different extracts exhibited distinct cytotoxicity profiles. Among all tested extracts, the hexane extract (GXBH) exhibited the highest cytotoxic activity, with IC₅₀ values of 66.9 ± 5.1 µg/mL (MDA-MB-231), 64.7 ± 14.9 µg/mL (Huh-7), 80.0 ± 11.9 µg/mL (A549), and 65.4 ± 7.8 µg/mL (SW480). In addition, GXBH significantly induced apoptosis and inhibited the colony-forming capability in all 4 cell lines. These findings highlight the potential of *G. xanthochymus* as a promising natural candidate for the development of alternative anticancer therapies.

Keywords: *Garcinia xanthochymus*, Anticancer activity, Cytotoxicity, Apoptosis, Colony-forming capability

Introduction

Garcinia xanthochymus Hook. f. is a medicinal plant widely distributed across Southeast Asia. It is a medium-sized perennial tree that reaches a height of approximately 10 - 20 m and is characterized by gray, thick bark and the production of opaque white resin [1].

Belonging to the Clusiaceae family [2], *G. xanthochymus* produces an edible yellow fruit that is commonly used in jams and occasionally in the production of vinegar, beverages, and other food products [3]. Phytochemical investigations have

revealed that the plant contains a variety of bioactive compounds, including xanthenes, flavonoids, and benzophenones. These metabolites are associated with a broad spectrum of biological activities, such as antioxidant, antibacterial, anti-inflammatory, antidiabetic, and anticancer effects [2,4-7], positioning *G. xanthochymus* as a potential source for pharmacological development.

Cancer remains a major global health challenge, with increasing incidence and mortality rates worldwide [8,9]. In 2022, approximately 20 million new cancer cases and 9.7 million cancer-related deaths were reported [10]. This burden is expected to rise significantly, with projections estimating 35 million new cases by 2050 [11]. According to the American Cancer Society (ACS), lung, breast, colorectal, and prostate cancers are among the most commonly diagnosed malignancies, accounting for an estimated 152,810 new cases in 2024 alone [12].

Given the urgent need for safer and more effective therapeutic options, natural products continue to be a valuable source for the discovery of anticancer agents [13]. This study aimed to evaluate the anticancer activity of crude extracts derived from *G. xanthochymus* against

4 human cancer cell lines. Extracts were prepared using a range of organic solvents, and their cytotoxic effects were assessed. Furthermore, the hexane extract (GXBH), which exhibited the most potent cytotoxicity, was selected for further investigation of its effects on apoptosis induction and colony-forming capability. The results of this study support the potential of *G. xanthochymus* as a promising candidate for the development of novel natural anticancer therapies.

Materials and methods

Preparation of crude extract

Barks, leaves, and twigs of *G. xanthochymus* were collected from Chiang Rai, Thailand. Dried barks (2.10 kg) were sequentially extracted with hexanes, dichloromethane, acetone, and methanol at room temperature, after evaporation, yielding GXBH (17.28 g), GXBD (25.48 g), GXBA (53.94 g), and GXBM (156.80 g). Dried leaves (2.10 kg) underwent the same process, yielding GXLH (17.22 g), GXLD (25.48 g), GXLA (57.94 g), and GXLM (156.81 g). Dried twigs (7.80 kg) yielded GXTH (9.42 g), GXTD (6.11 g), GXTA (70.54 g), and GXTM (125.09 g) (**Figure 1**).

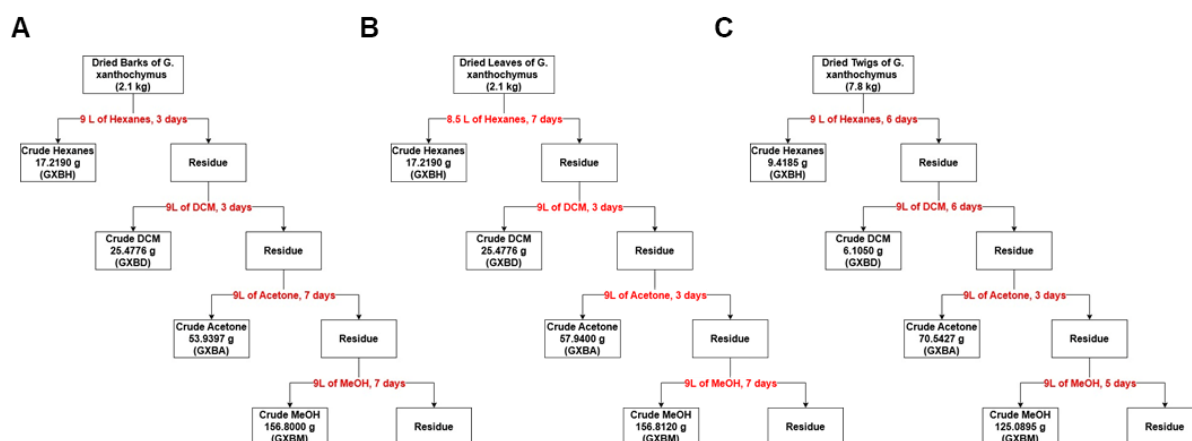


Figure 1 The extraction scheme of (A) barks, (B) leaves, and (C) twigs of *G. xanthochymus* with organic solvent hexanes, dichloromethane (DCM), acetone, and methanol (MeOH).

UHPLC-QTOF Analysis

Each crude extract was dissolved in chromatographic-grade methanol to a final concentration of 0.2 mg/mL. The solutions were filtered through a 0.22 μ m, 13 mm Nylon syringe filter and transferred to 2 mL autosampler vials. Ultra-high-

performance liquid chromatography coupled with quadrupole time-of-flight (UHPLC-QTOF) mass spectrometry analysis was performed using an Agilent 1290 Infinity II system equipped with a 6545B QTOF mass spectrometer and a Dual AJS ESI source operating

in positive ion mode (Agilent Technologies, Santa Clara, CA, USA).

A 1.00 μL sample was injected and separated on an Agilent Poroshell 120 EC-C18 column ($2.1 \times 150 \text{ mm}^2$, $2.7 \mu\text{m}$) maintained at 35°C with a flow rate of 0.2 mL/min . The mobile phase consisted of (A) 0.1% v/v formic acid in water and (B) 0.1% v/v formic acid in acetonitrile. Gradient elution was performed as follows: 0 - 1 min, 95% A; 1 - 13 min, 83% A; 13 - 25 min, 5% A; 25 - 33 min, 95% A.

Mass spectrometry data were acquired in AutoMS2 mode using fixed collision energies of 10.0, 20.0, and 40.0 V. The MS scan range was set to m/z 100 - 1100 with a scan rate of 3.0 spectra/s, and the MS/MS range was m/z 50 - 1100 with the same scan rate. The nebulizer pressure was maintained at 35 psig, with a drying gas temperature of 300°C and a flow rate of 10 L/min . The sheath gas was set at 350°C with a flow rate of 11 L/min . The fragmentor voltage was 175 V, capillary voltage 3500 V, and nozzle voltage 1000 V.

Cell culture

Human cancer cell lines MDA-MB-231 (breast; HTB-26, American Type Culture Collection (ATCC), Manassas, VA, USA), Huh-7 (liver; JCRB0403, Japanese Collection of Research Bioresources (JCRB), Osaka, Japan), A549 (lung; CCL-185, ATCC), and SW480 (colon; CCL-228, ATCC) were cultured in Dulbecco's modified Eagle medium (DMEM; Gibco, Thermo Fisher Scientific Inc.) with 10% fetal bovine serum (FBS; Gibco, Thermo Fisher Scientific Inc.) and 1% penicillin-streptomycin solution (Gibco, Thermo Fisher Scientific Inc.). The cells were maintained at 37°C in a humidified atmosphere containing 5% CO_2 . Subculturing was performed at 90% confluence using standard trypsinization methods. Cell viability and counting were assessed using trypan blue exclusion staining.

Cytotoxicity assay

Cell cytotoxicity was determined using the standard 3-[4,5 dimethylthiazol-2-yl]-2,5 diphenyl tetrazolium bromide assay (MTT assay) with modifications [14]. MDA-MB-231, Huh-7, A549, and SW480 cells (2×10^4 cells/well) were seeded into 96-well plates and incubated for 24 h. Cells were treated with GX crude extracts (200 - $12.5 \mu\text{g/mL}$) for 72 h.

Untreated and 1% Dimethyl Sulfoxide (DMSO; PanReac AppliChem, Darmstadt, Germany) solvent controls were included. Following, $10 \mu\text{L}$ of MTT solution (5 mg/mL) was added to each well, and the plates were incubated for 1 h. Formazan crystals were dissolved in $100 \mu\text{L}$ DMSO, and OD was measured at 570 nm. Cell viability was calculated, and IC_{50} values were determined using GraphPad Prism 10.1.2 (GraphPad Software, Inc., San Diego, California).

Apoptosis assay

The apoptosis assay was conducted using the Annexin V-FITC Apoptosis Staining/Detection Kit (ab14085, Abcam, Cambridge, UK) as described previously [15,16]. Briefly, MDA-MB-231, Huh-7, A549, and SW480 cells (2×10^5 cells/well) were seeded into 24-well culture plates and incubated for 24 h. Thereafter, the cells were treated with $100 \mu\text{g/mL}$ of GXBH for 96 h. After treatment, the cells were collected by trypsinization and washed with PBS. The cells were stained with annexin V-FITC and PI solution and analyzed using the Dx FLEX flow cytometer (Beckman Coulter Inc., IN, USA). The percentages of live cells (Annexin V-/PI-), early apoptotic cells (Annexin V+/PI-), and late apoptotic cells (Annexin V+/PI+) were quantified using the CytExpert for Dxflex software (Beckman Coulter Inc.).

Colony formation assay

MDA-MB-231, Huh-7, A549, and SW480 cells (2×10^4 cells/well) were seeded in 96-well plates and incubated for 24 h. Cells were treated with $100 \mu\text{g/mL}$ of GXBH for 96 h, followed by trypsinization and cell counting. Viable cells (1×10^3 for MDA-MB-231 and 5×10^3 for the other cell lines) were transferred to 12-well plates and incubated for colony formation (3 days for Huh-7 and 4 days for the other cell lines). The colonies were fixed with cool methanol, stained with 0.5% crystal violet overnight, photographed, and analyzed using ImageJ software (National Institutes of Health, Bethesda, USA).

Statistical analysis

Each experiment was performed in triplicate, and the data are presented as mean \pm standard deviation (SD). Statistical analysis was conducted using one-way analysis of variance (ANOVA), followed by Turkey's

post hoc test, using GraphPad Prism 10.1.2 (GraphPad Software, Inc.). A *P*-value of less than 0.05 was considered statistically significant.

Results and discussion

Metabolites in different parts of *G. xanthochymus*

xanthochymus

The metabolite profiles of crude extracts from different parts of *G. xanthochymus* are presented in a bar graph (Figure 2). The major compound groups identified include xanthenes, flavonoids, and other classes such as benzophenones, phloroglucinols, polyphenols, coumarins, and organic acids. In total, 73 metabolites were identified across all extracts, comprising 36 xanthenes, 37 flavonoids, and 29 metabolites from other compound groups (Table S1). Xanthenes were unevenly distributed among the extracts. Notably, compounds 45, 50, and 55 were highly abundant in GXBM and GXTA, while GXTM also exhibited a high xanthone content but with a distinct profile compared to the other extracts. This variation suggests that GXBM and GXTA possess a greater capacity for xanthone biosynthesis, potentially influenced by genetic factors or environmental conditions. Flavonoids, represented by 37 identified metabolites, were more uniformly distributed across the extracts than xanthenes. Extracts such as GXLA, GXLD, and GXTH contained moderate to high levels of various flavonoids. However, none of the extracts exhibited flavonoid levels as high as those observed for

xanthenes, suggesting that flavonoid production in *G. xanthochymus* may be more consistent and less variable. The remaining 29 metabolites—including benzophenones, phloroglucinols, polyphenols, coumarins, and organic acids—were generally present in lower abundance. Nonetheless, GXLD and GXTA showed elevated levels of certain metabolites, indicating selective accumulation. This selectivity may reflect specialized metabolic processes or be influenced by external factors such as environmental conditions. These findings are consistent with previous reports indicating that *Garcinia* species are prolific producers of xanthenes and flavonoids. The observed patterns of metabolite accumulation are likely regulated by both genetic and environmental factors [2,17-19]. Regarding bioavailability, *G. xanthochymus* is recognized for its pharmacological potential, primarily due to the presence of xanthenes, benzophenones, and flavonoids; however, further studies are required to fully elucidate their bioavailability and mechanisms of action [2]. In 2020, Janhavi *et al.* [20] reported that polyphenols such as epicatechin and catechin isolated from *G. xanthochymus* fruit exhibited high bioaccessibility and bioavailability. *In vivo* studies in mice demonstrated that peak plasma concentrations (C_{max}) were reached approximately 2 h following oral administration [20]. These findings indicate that *G. xanthochymus* is a promising source of bioavailable antioxidant compounds with potential applications in functional foods and pharmaceuticals.

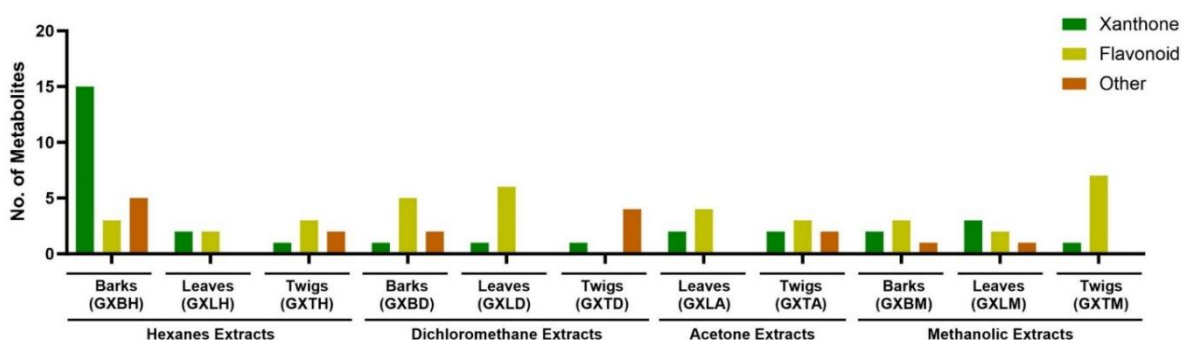


Figure 2 Metabolite distribution in *G. xanthochymus* crude extracts. A bar graph shows the number of xanthone, flavonoid, and other identified in crude extracts from each part in different solvents.

Cytotoxicity effect of *G. xanthochymus* crude extract on cancer cell lines

The cytotoxic activities of *G. xanthochymus* crude extracts—prepared using hexanes, dichloromethane, acetone, and methanol—were evaluated against 4 human cancer cell lines: MDA-MB-231 (breast cancer), Huh-7 (liver cancer), A549 (lung cancer), and SW480 (colon cancer). As shown in the bar graphs (Figures 3(A), 3(C), 3(E), and 3(G)), the hexanes and dichloromethane extracts exhibited strong cytotoxic effects, particularly against MDA-MB-231 and SW480 cells. In contrast, extracts prepared with acetone and methanol demonstrated comparatively lower cytotoxicity. A dose-dependent reduction in cell viability was observed across all tested cell lines.

The heat maps (Figures 3(B), 3(D), 3(F), and 3(H)) revealed distinct cytotoxic response patterns for each cell line, suggesting that differences in extract composition may influence cellular sensitivity. These cytotoxic effects are likely attributable to bioactive secondary metabolites such as xanthenes, flavonoids, and benzophenones found in *G. xanthochymus* [2,4-7]. The IC₅₀ values for each extract are summarized in Table 1. Among all extracts, the hexane extract (GXBH) demonstrated the highest cytotoxic activity, with IC₅₀ values of 66.9 ± 5.1 µg/mL for MDA-MB-231, 64.7 ± 14.9 µg/mL for Huh-7, 80.0 ± 11.9 µg/mL for A549, and 65.4 ± 7.8 µg/mL for SW480 cells. Based on these results, GXBH was selected for further studies to investigate its effects on apoptosis and colony-forming ability.

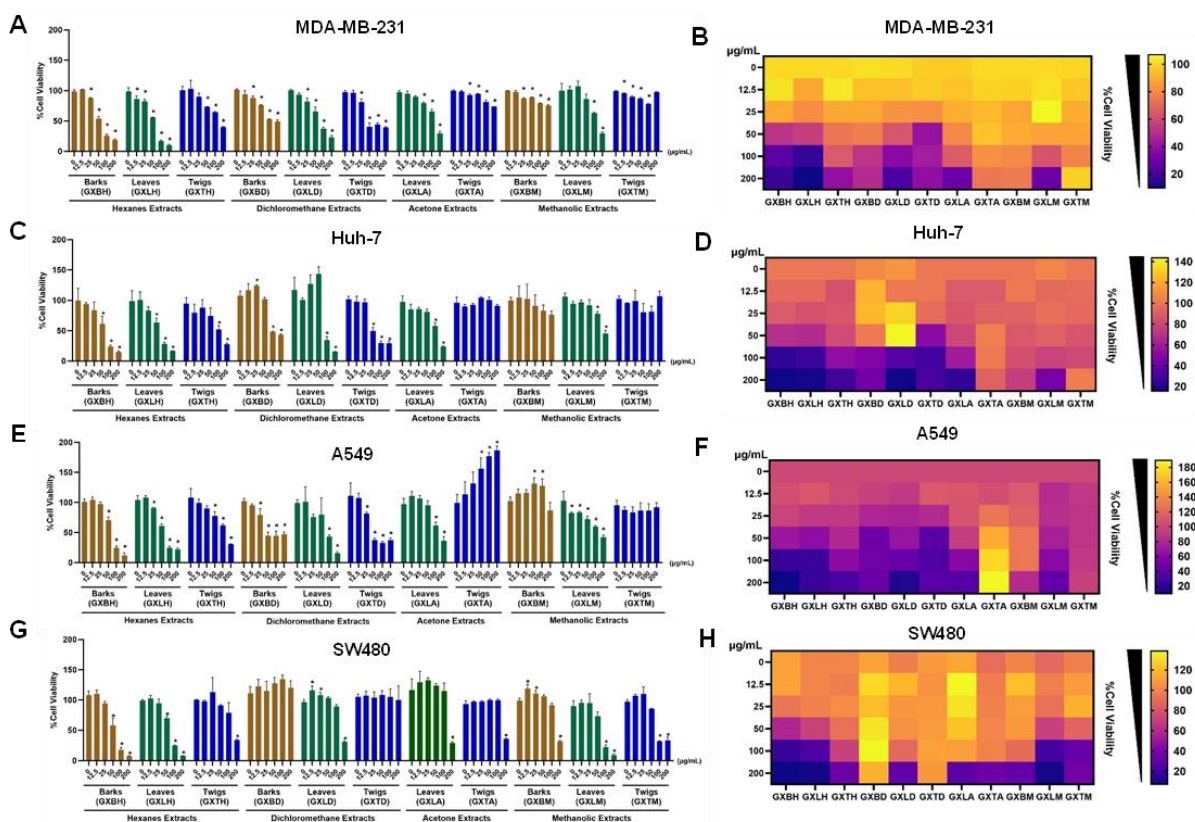


Figure 3 Cytotoxicity assay of human cancer cell lines after treatment with *G. xanthochymus* crude extracts for 72 h. Bar graphs show the percentage of cell viability of MDA-MB-231 (A), Huh-7 (C), A549 (E), and SW480 (G). Data represents SD from 3 independent experiments. **P* < 0.05 vs. equivalent concentrations of vehicle solvent (DMSO). Heat maps illustrate the percentage of cell viability in MDA-MB-231 (B), Huh-7 (D), A549 (F), and SW480 (H).

Table 1 Anti-cancer effect of hexanes, dichloromethane, acetone, and methanolic crude extracts of *G. xanthochymus* to against 4 human cancer cells.

Crude	Cell lines (IC ₅₀ - µg/mL)			
	MDA-MB-231	Huh-7	A549	SW480
GXBH	66.9 ± 5.1	64.7 ± 14.9	80.0 ± 11.9	65.4 ± 7.8
GXLH	51.7 ± 2.8	71.1 ± 11.6	76.9 ± 3.9	75.0 ± 3.8
GXTH	162.6 ± 6.2	109.6 ± 38.8	143.7 ± 18.8	212.5 ± 27.6
GXBD	154.4 ± 2.0	228.2 ± 12.9	89.0 ± 22.1	Inactive
GXLD	80.2 ± 10.1	188.0 ± 25.7	92.9 ± 27.2	297.6 ± 19.0
GXTD	77.4 ± 3.5	76.3 ± 6.8	69.5 ± 9.9	Inactive
GXLA	148.0 ± 2.0	118.4 ± 14.5	210.3 ± 39.6	524.0 ± 12.8
GXTA	539.0 ± 27.8	Inactive	Inactive	323.0 ± 20.5
GXBM	482.4 ± 19.0	Inactive	Inactive	323.5 ± 21.2
GXLM	173.7 ± 11.6	259.4 ± 41.5	137.8 ± 17.3	73.7 ± 3.7
GXTM	Inactive	Inactive	Inactive	130.6 ± 7.3

Effect of GXBH extract on apoptosis of cancer cells

Apoptosis is a fundamental process in the elimination of cancer cells and a key target in anticancer therapy [21]. To assess the pro-apoptotic effects of the GXBH extract, annexin V and propidium iodide (PI) staining were performed on 4 cancer cell lines. The initial experimental conditions were based on IC₅₀ concentrations and time points determined from cytotoxicity assays. However, annexin V/PI staining revealed less than 10% apoptosis under these conditions. To improve the detection of apoptosis, the treatment concentration was increased to 100 µg/mL, resulting in approximately 90% cell death, and the incubation period was extended to 96 h. Our results revealed a significant increase in the proportion of apoptotic cells in all cell lines treated with GXBH compared to untreated controls (**Figures 4(A) - 4(H)**). Notably, the SW480 cell line exhibited a marked elevation in early apoptotic cells (**Figures 4(G) and 4(H)**), highlighting the potential of GXBH to trigger apoptosis in cancer cells.

The varying ratios of early and late apoptotic populations across different cell lines may be attributed

to differential expression of key apoptosis-regulating proteins, such as Bcl-2, Bax, and members of the caspase family [22,23]. These proteins play central roles in the intrinsic and extrinsic apoptotic pathways and may modulate the cellular response to GXBH treatment. Xanthones have long been recognized as natural anti-cancer agents [24]. Mechanistically, they induce apoptosis primarily via the mitochondrial (intrinsic) pathway, characterized by decreased intracellular ATP levels, release of cytochrome c and apoptosis-inducing factor (AIF), activation of caspase-9 and caspase-3, and translocation of endonuclease G. In addition, xanthones modulate apoptosis through the miR-143/ERK5/c-Myc signaling axis, inhibit nitric oxide production (NO), induce cell cycle arrest, inhibit sarco/endoplasmic reticulum Ca²⁺-ATPase (SERCA), and promote the accumulation of intracellular reactive oxygen species (ROS) [25]. Nevertheless, further mechanistic studies are required to elucidate the specific molecular pathways by which GXBH induces apoptosis in cancer cells.

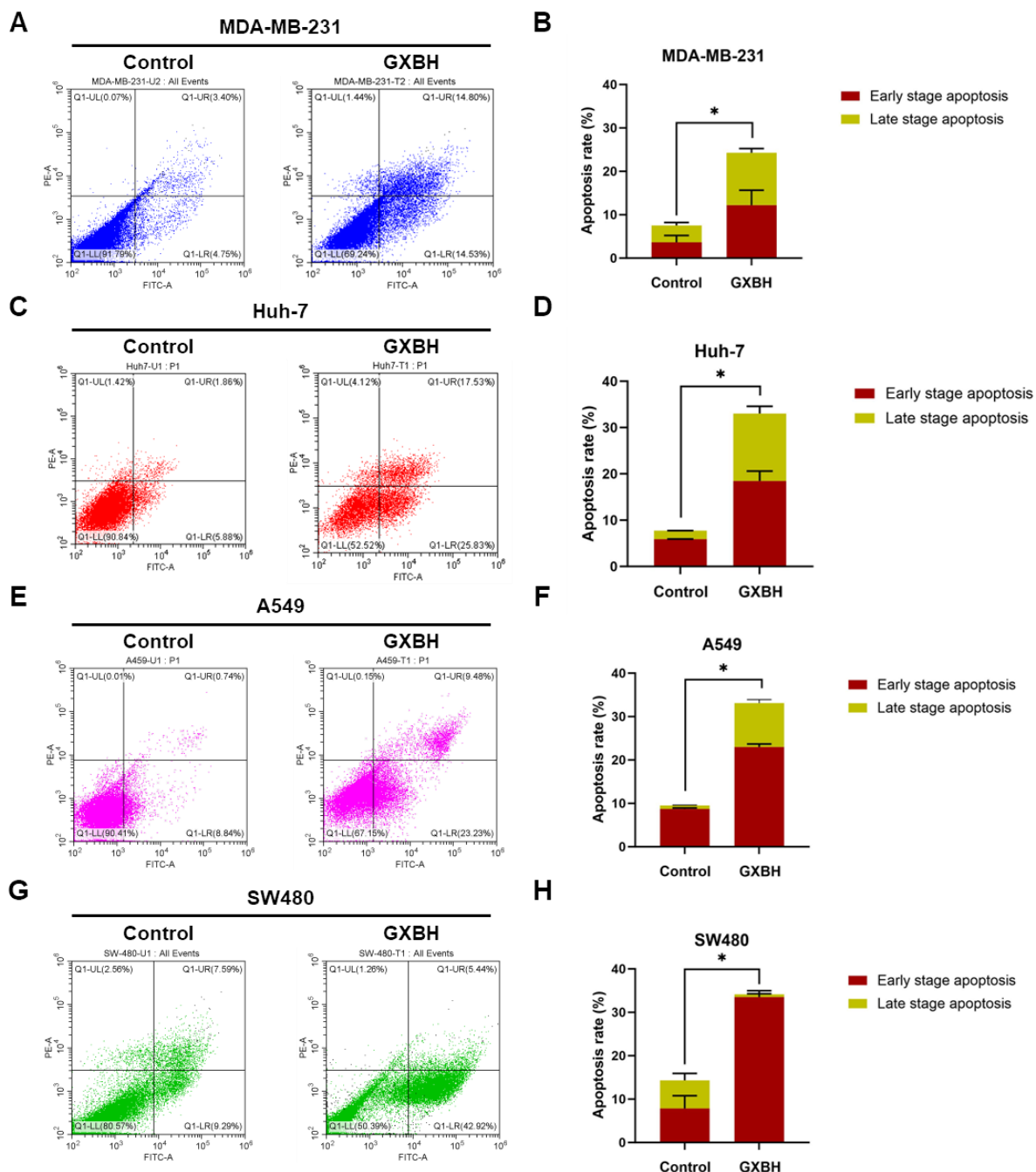


Figure 4 Annexin V and PI staining assay of human cancer cell lines after treatment with GXBH for 96 h. Representative flow cytometric dot plots of annexin V and PI-stained cells in MDA-MB-231 (A), Huh-7 (C), A549 (E), and SW480 (G). Bar graphs show the percentage of apoptotic cells in MDA-MB-231 (B), Huh-7 (D), A549 (F), and SW480 (H). Data represent mean \pm SD from 3 independent experiments. * $P < 0.05$ vs. control (0 μ g/mL).

Effect of GXBH extract on colony-forming capability

Colony-forming capability is a hallmark of cancer, reflecting the uncontrolled proliferative potential of cancer cells [26]. The anti-colony-forming effect of GXBH was assessed across 4 cancer cell lines by quantifying the percentage of colony area intensity.

Compared to the untreated control, GXBH significantly inhibited colony formation, particularly in A549 and MDA-MB-231 cells (Figures 5(A) and 5(B)), suggesting a possible selectivity of GXBH toward specific cancer types. The observed reduction in colony-forming ability indicates the potential of GXBH to suppress long-term cancer cell growth, correlating with

its pro-apoptotic effects. GXBH not only induces apoptosis but also exhibits anti-proliferative activity. The significant decrease in colony-forming ability may be attributed to the inhibition of cyclin-dependent kinases (CDKs), which regulate the S and M phases of the cell cycle, or to the upregulation of CDK inhibitors such as p21 and p27 [27,28]. Previous studies have

reported that compounds isolated from *Garcinia* species exhibit diverse biological activities, including the inhibition of multiple signaling pathways. GXBH may similarly suppress cancer cell growth by targeting PI3K/Akt/mTOR or MAPK/ERK signaling pathways [29,31].

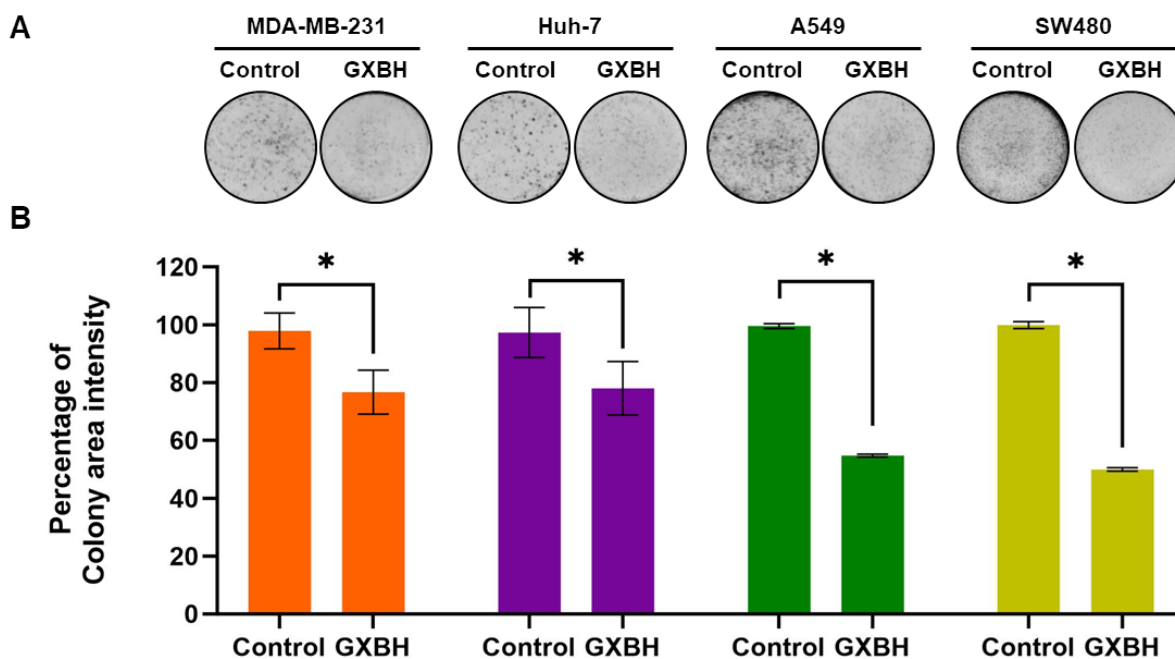


Figure 5 Clonogenic assay of human cancer cell lines after treatment with GXBH for 96 h. (A) Representative images of formed colonies of MDA-MB-231, Huh-7, A549, and SW480. (B) Bar graphs show the percentage of colony area intensity of MDA-MB-231, Huh-7, A549, and SW480. Data represent mean \pm SD from 3 independent experiments. * $P < 0.05$ vs. control (0 $\mu\text{g/mL}$).

Conclusions

In summary, this study demonstrates that the crude extract of *G. xanthochymus*, particularly the hexanes extract (GXBH), exhibits significant anticancer activity against multiple cancer cell lines. GXBH effectively induces apoptosis and suppresses colony-forming ability, underscoring its potential as a promising natural anticancer agent. Nevertheless, further research is required to elucidate the molecular mechanisms underlying its anticancer effects. Comprehensive studies on its safety profile, pharmacokinetics, and *in vivo* efficacy are also essential to evaluate its potential for clinical development.

Acknowledgements

We would like to thank Mae Fah Luang University for providing a postgraduate scholarship and overseas training support to Mr. Sirachuch Maungprasert, as well as for access to laboratory facilities.

Declaration of Generative AI in Scientific Writing

The authors acknowledge the use of generative AI tools (e.g., QuillBot and ChatGPT by OpenAI) in the preparation of this manuscript, specifically for language editing and grammar correction. No content generation or data interpretation was performed by AI. The authors take full responsibility for the content and conclusions of this work.

CRedit Author Statement

Sirachuch Maungprasert: Statistical analysis, Formal analysis, Investigation, Writing – original draft preparation.

Wim Vanden Berghe: Supervision, Writing – review & editing.

Chung Sub Kim: Supervision, Resources, Writing – review and editing.

Surat Laphookhieo: Conceptualization, Project administration, Supervision, Resources, Writing – review & editing.

Keerakarn Somsuan: Resources, Visualization, Writing – review & editing.

Siripat Aluksanasuwan: Resources, Visualization, Writing – review & editing.

Atthapan Morchang: Conceptualization, Methodology, Statistical analysis, Formal analysis, Investigation, Resources, Visualization, Writing – review & editing.

Suwanna Deachathai: Conceptualization, Methodology, Visualization, Supervision, Resources, Writing - review and editing.

References

- [1] F Ji, Z Li, G Liu, S Niu, N Zhao, X Liu and H Hua. Xanthones with antiproliferative effects on prostate cancer cells from the stem bark of *Garcinia xanthochymus*. *Natural Product Communications* 2012; **7(1)**, 53-56.
- [2] NKN Che Hassan, M Taher and D Susanti. Phytochemical constituents and pharmacological properties of *Garcinia xanthochymus* - A review. *Biomedicine and Pharmacotherapy* 2018; **106**, 1378-1389.
- [3] J Prakash, S Sallaram, A Martin, RP Veeranna and MS Peddha. Phytochemical and functional characterization of different parts of the *Garcinia xanthochymus* fruit. *ACS Omega* 2022; **7(24)**, 21172-21182.
- [4] X He, F Yang and X Huang. Proceedings of chemistry, pharmacology, pharmacokinetics and synthesis of biflavonoids. *Molecules* 2021; **26(19)**, 6088.
- [5] M Hemshekhar, K Sunitha, MS Santhosh, S Devaraja, K Kemparaju, BS Vishwanath, SR Niranjana and KS Girish. An overview on genus *garcinia*: Phytochemical and therapeutical aspects. *Phytochemistry Reviews* 2011; **10(3)**, 325-351.
- [6] S Baggett, P Protiva, EP Mazzola, H Yang, ET Ressler, MJ Basile, IB Weinstein and EJ Kennelly. Bioactive benzophenones from *Garcinia xanthochymus* fruits. *Journal of Natural Products* 2005; **68(3)**, 354-360.
- [7] Y Chen, F Zhong, H He, Y Hu, D Zhu and G Yang. Structure elucidation and NMR spectral assignment of five new xanthones from the bark of *Garcinia xanthochymus*. *Magnetic Resonance in Chemistry* 2008; **46(12)**, 1180-1184.
- [8] MC García, LM Rossen, K Matthews, G Guy, KF Trivers, CC Thomas, L Schieb and MF Iademarco. Preventable premature deaths from the five leading causes of death in nonmetropolitan and metropolitan counties, united states, 2010 - 2022. *MMWR Surveillance Summaries* 2024; **73(2)**, 1-11.
- [9] RR Tourinho-Barbosa, ACL Pompeo and S Glina. Prostate cancer in Brazil and Latin America: Epidemiology and screening. *International Brazilian Journal of Urology* 2016; **42(6)**, 1081-1090.
- [10] HM Bizuayehu, KY Ahmed, GD Kibret, AF Dadi, SA Belachew, T Bagade, TK Tegegne, RLVencharutti, KT Kibret, AH Hailegebireal, Y Assefa, MN Khan, A Abajobir, KA Alene, Z Mengesha, D Erku, DA Enquobahrie, TZ Minas, E Misgan and AG Ross. Global disparities of cancer and its projected burden in 2050. *JAMA Network Open* 2024; **7(11)**, e2443198.
- [11] World Health Organization (WHO), Available at: <https://www.who.int/news/item/01-02-2024-global-cancer-burden-growing--amidst-mounting-need-for-services>, accessed March 2025.
- [12] RL Siegel, AN Giaquinto and A Jemal. Cancer statistics, 2024. *CA: A Cancer Journal for Clinicians* 2024; **74(1)**, 12-49.
- [13] AG Atanasov, SB Zotchev, VM Dirsch and CT Supuran. Natural products in drug discovery: Advances and opportunities. *Nature Reviews Drug Discovery* 2021; **20(3)**, 200-216.
- [14] JV Meerloo, GJL Kaspers and J Cloos. Cell sensitivity assays: The MTT assay. *Methods in Molecular Biology* 2011; **731**, 237-245.

- [15] S Aluksanasuwan, K Somsuan, W Chiangjong, A Rongjumnong, W Jaidee, N Rujanapun, S Chutipongtanate, S Laphookhieo and R Charoensup. SWATH-proteomics reveals Mathurameha, a traditional anti-diabetic herbal formula, attenuates high glucose-induced endothelial dysfunction through the EGF/NO/IL-1 β regulatory axis. *Journal of Proteomics* 2024; **306**, 105263.
- [16] S Aluksanasuwan, K Somsuan, J Ngoenkam, W Chiangjong, A Rongjumnong, A Morchang, S Chutipongtanate and S Pongcharoen. Knockdown of heat shock protein family D member 1 (HSPD1) in lung cancer cell altered secretome profile and cancer-associated fibroblast induction. *BBA Molecular Cell Research* 2024; **1871(5)**, 119736.
- [17] JM Kumatso and G Sigge. Nutritional benefits, phytoconstituents, and pharmacological properties of *Garcinia* fruits: A review. *Biointerface Research in Applied Chemistry* 2024; **14(5)**, 102.
- [18] P Pailee, T Kruahong, S Hongthong, C Kuhakarn, T Jaipetch, M Pohmakotr, S Jariyawat, K Suksen, R Akkarawongsapat, J Limthongkul, A Panthong, P Kongsaeere, S Prabpai, P Tuchinda and V Reutrakul. Cytotoxic, anti-HIV-1 and anti-inflammatory activities of lanostanes from fruits of *Garcinia speciosa*. *Phytochemistry Letters* 2017; **20**, 111-118.
- [19] V Reutrakul, N Anantachoke, M Pohmakotr, T Jaipetch, S Sophasan, C Yoosook, J Kasisit, C Napaswat, T Santisuk and P Tuchinda. Cytotoxic and anti-HIV-1 caged xanthenes from the resin and fruits of *Garcinia hanburyi*. *Planta Medica* 2006; **73(1)**, 33-40.
- [20] P Janhavi, S Sindhoora and SP Muthukumar. Bioaccessibility and bioavailability of polyphenols from sour mangosteen (*Garcinia xanthochymus*) fruit. *Journal of Food Measurement and Characterization* 2020; **14(7)**, 2414-2423.
- [21] S Elmore. Apoptosis: A review of programmed cell death. *Toxicologic Pathology* 2007; **35(4)**, 495-516.
- [22] V Papaliagkas, A Anogianaki, G Anogianakis and G Ilonidis. The proteins and the mechanisms of apoptosis: A mini-review of the fundamentals. *Hippokratia* 2007; **11(3)**, 108-113.
- [23] S Qian, Z Wei, W Yang, J Huang, Y Yang and J Wang. The role of BCL-2 family proteins in regulating apoptosis and cancer therapy. *Frontiers in Oncology* 2022; **12**, 985363.
- [24] YS Kurniawan, KTA Priyanga, Jumina, HD Pranow, EN Sholikhah, AK Zulkarnain, HA Fatimi and J Julianus. An update on the anticancer activity of xanthone derivatives: A review. *Pharmaceuticals* 2021; **14(11)**, 1144.
- [25] T Shan, Q Ma, K Guo, J Liu, W Li, F Wang and E Wu. Xanthenes from mangosteen extracts as natural chemopreventive agents: Potential anticancer drugs. *Current Molecular Medicine* 2011; **11(8)**, 666-677.
- [26] D Hanahan and RA Weinberg. Hallmarks of cancer: The next generation. *Cell* 2011; **144(5)**, 646-674.
- [27] J Zhang, G Su, Y Lin, W Meng, JKL Lai, L Qiao, X Li and X Xie. Targeting cyclin-dependent kinases in gastrointestinal cancer therapy. *Discovery Medicine* 2019; **27(146)**, 27-36.
- [28] J Patel, HY Wong, W Wang, J Alexis, A Shafiee, AJ Stevenson, B Gabrielli, NM Fisk and K Khosrotehrani. Self-renewal and high proliferative colony forming capacity of late-outgrowth endothelial progenitors is regulated by cyclin-dependent kinase inhibitors driven by notch signaling. *Stem Cells* 2016; **34(4)**, 902-912.
- [29] J Xu, S Jin, F Gan, H Xiong, Z Mei, Y Chen and G Yang. Polycyclic polyprenylated acylphloroglucinols from *Garcinia xanthochymus* fruits exhibit antitumor effects through inhibition of the STAT3 signaling pathway. *Food and Function* 2020; **11(12)**, 10568-10579.
- [30] MM Patil and KAK Appaiah. *Garcinia: Bioactive compounds and health benefits*. Food Science Publisher, Dallas, 2015, p. 110-125.
- [31] A Paul and MK Zaman. A comprehensive review on ethnobotany, nutritional values, phytochemistry and pharmacological attributes of ten *Garcinia* species of South-east Asia. *South African Journal of Botany* 2022; **148**, 39-59.